SUPERNOVA REMNANTS II
AN ODYSSEY IN SPACE AFTER STELLAR DEATH
3-8 June 2019, Chania, Crete, Greece

Measuring the post-shock temperatures of heavy ions in SN 1987A

Marco Miceli

Dipartimento di Fisica e Chimica, Università di Palermo

INAF – Osservatorio Astronomico di Palermo

Collaborators: S. Orlando, D. Burrows, S. Park, A. Pazhayath-Ravi, K. Frank, C. Argiroffi, F. Bocchino, O. Petruk, E. Greco, G. Peres

Collisionless shocks

Rankine-Hugoniot conditions predict that the post-shock temperature depends on the shock velocity v_s as

$$kT = 3/16\ m v_s^2$$

In astrophysical shocks **particle–particle interactions (Coulomb collisions) cannot determine the viscous dissipation**, and collective effects provide the jump conditions.

Collisionless shocks in a plasma with different particle species

complete equilibration → $kT = 3/16\ \mu m_p v_s^2$

Everything in between is possible

full non-equilibration → $kT_i = 3/16\ m_i v_s^2$

Collisionless shocks are ubiquitous and SNRs are ideal targets because of their bright post-shock emission and fast shocks

Collisionless shocks – electrons and protons

In SNRs $T_e/T_p > m_e/m_p$ and can increase up to 1 in slow shocks, with $T_e/T_p \propto v_s^{-2}$.
This can be explained if **T_e does not depend on v_s** ($kT_e \sim 0.3$ keV), **and $T_p \propto v_s^2$**: lower hybrid waves model (Ghavamian et al. 2007 but see also the thermodynamic explanation in Vink et al. 2015)

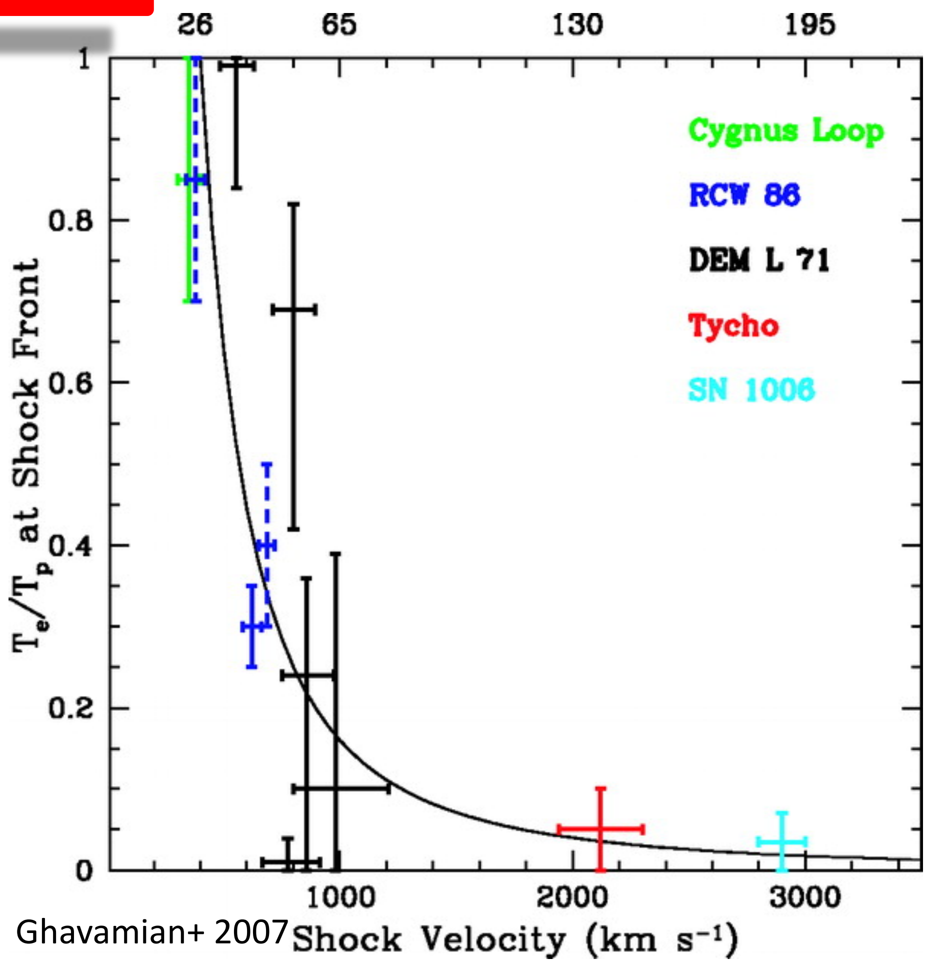

Ghavamian+ 2007

In general, there can be different plasma instabilities that can enhance Te/Tp and the **electron heating processes in collisionless shocks are different from those of ions** (Park, Caprioli, & Spitkovsky 2017, Bykov+2008, Shimada&Hoshino 2000)

Collisionless shocks – Ions

If different species react independently to the shock $kT_i \propto m_i v_s^2$

The measure of kT_i for different ions has produced contradictory results:

- $T_O/T_p < m_O/m_p$ (UV observations of SN 1006, Korreck et al. 2004)
- $T_O/T_p > m_O/m_p$ (interplanetary shock, Berdichevsky et al. 1997)
- $T_i/T_p \approx m_i/m_p$ (for He, C, N, UV obs of SN 1006, Raymond et al. 2017)

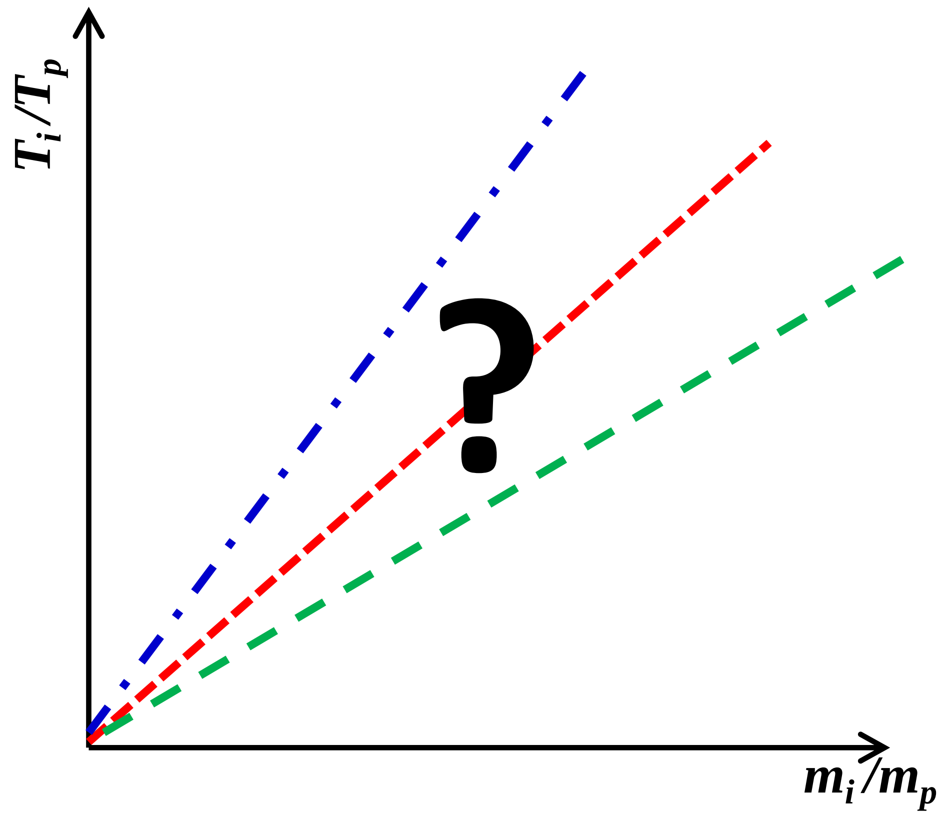

Collisionless shocks – Ions

It is necessary to extend the analysis over **a wider range of masses** to get tight constraints (heavy ions ➡ **X-ray band**).

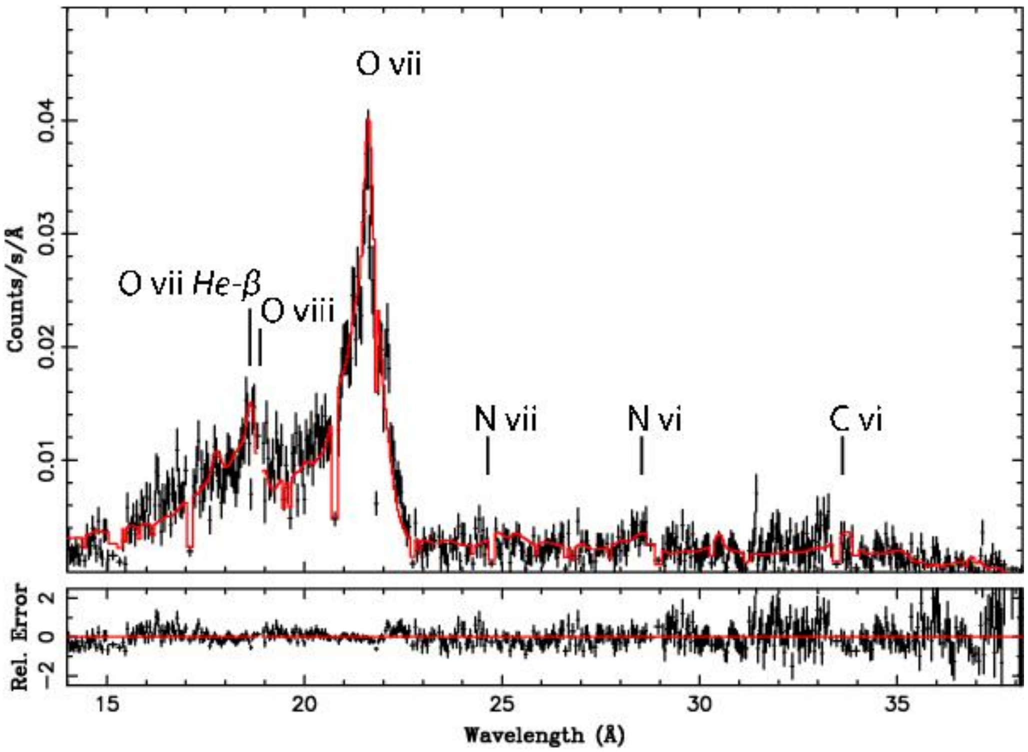

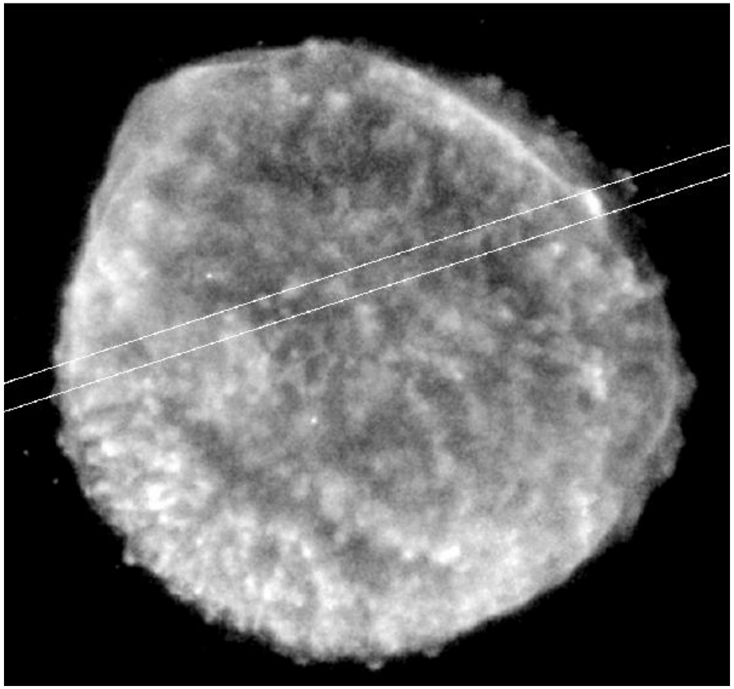

Line broadening of the OVII line triplet, corresponding to an **extremely high O temperature (~300 keV)** in an isolated ejecta knot of **SN 1006** (Vink et al. 2003, Broersen et al. 2013).

X-ray observations of SN 1987A

We focus on **SN 1987A** to study the ion heating at its shocks. This is an ideal target because of the **continuous monitoring** with X-ray (and multi-λ) observatories to follow the transition from a SN to a SNR

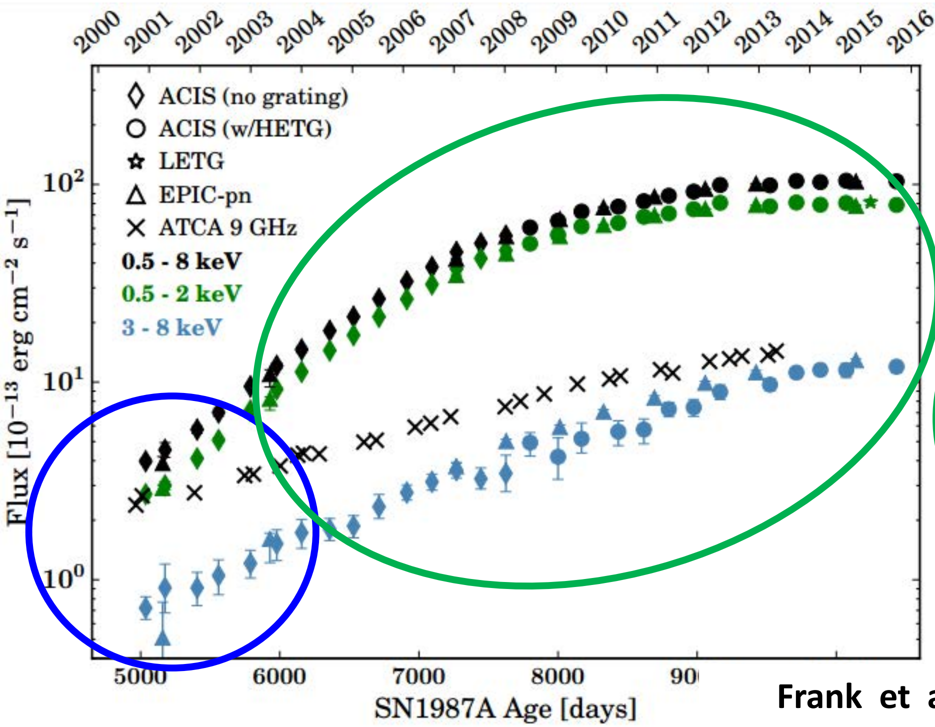

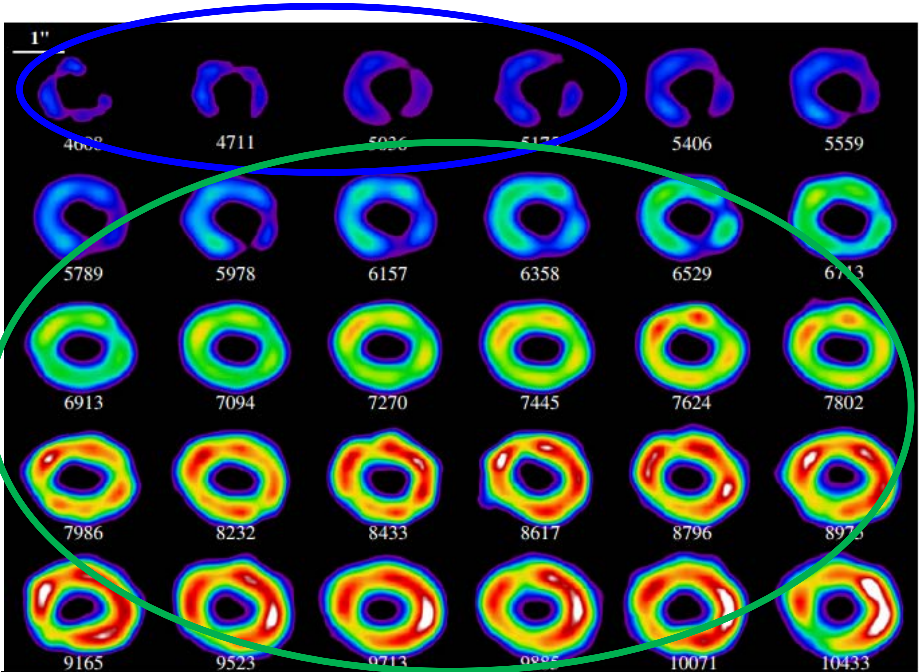

Frank et al. 2016

X-ray lightcurves and high-resolution images reflect the complex interaction with the multi-phase circumstellar material characterized by

1. A tenuous (10^2 cm^{-3}) HII region with hard X-ray thermal emission
2. A circumstellar dense (10^3 cm^{-3}) equatorial ring with knots (10^4 cm^{-3}), with soft X-ray emission

Our approach

Current models of the X-ray spectra of SN 1987A are *phenomenological* (*ad hoc* isothermal components) and analyze single observations, regardless of the whole succession of data sets (ignoring information embedded in the data)

We perform **3-D hydrodynamic simulations** to model the evolution of SN 1987A with a forward modeling approach

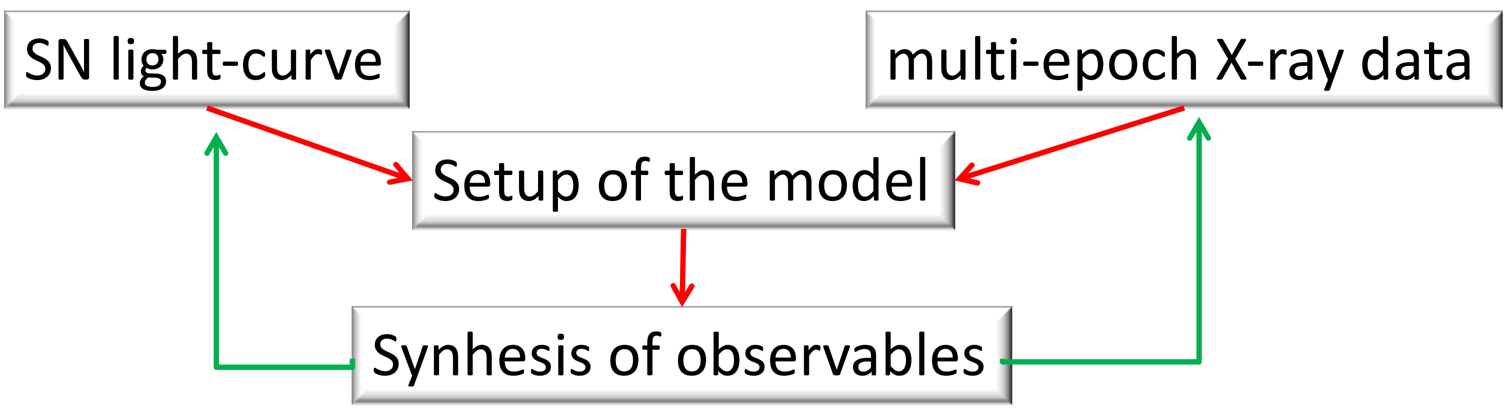

This approach aims at understanding the physical origin of the emission and of its evolution through a unique physical model

Initial conditions and parameter space

Orlando+ 2015 (see S. Orlando's talk and poster S2.3 by F. Bocchino)

- Clumping of ejecta
- Radiative losses from optically thin plasma
- Non-equilibrium of ionization
  - time evolution of each parcel of gas is followed (Dwarkadas+ 2010)
  - deviations from equilibrium of selected element (O, Ne, Mg, Si) is calculated
- Tracers to follow the evolution of ejecta, HII region, and ring material

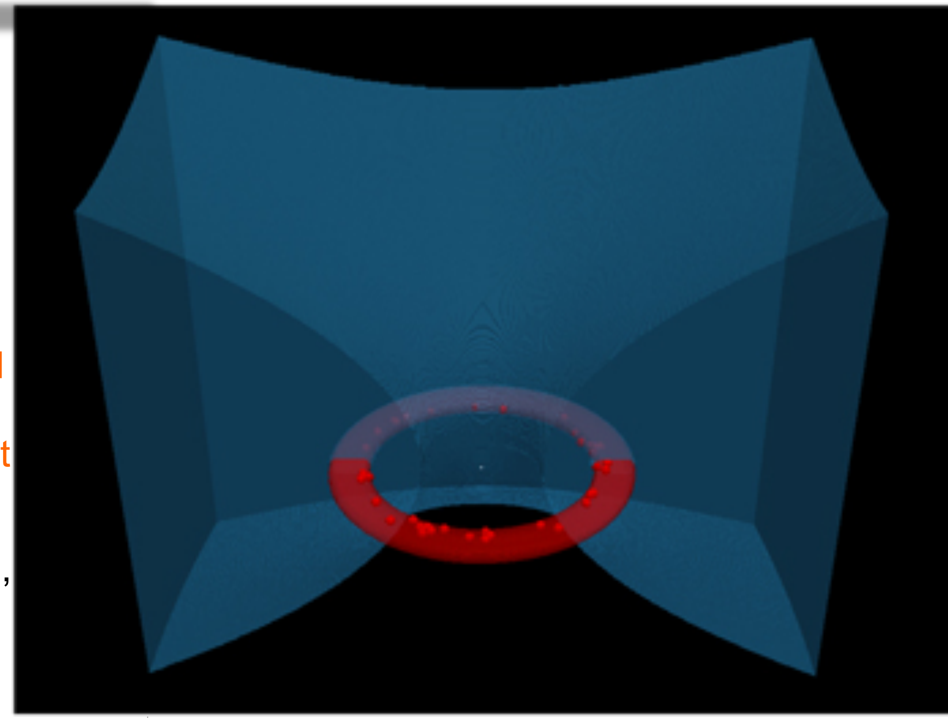

Spatial resolution

- Initial remnant radius ~ 20 AU (3e14 cm)
- Full spatial domain ~ 1 pc (3e18 cm)

18 nested levels of adaptive mesh refinement
effective resolution ~ 0.2 AU (3e12 cm)

> 100 cells per remnant radius during the whole evolution

			range of values explored	best-fit values
HII reg.	n_{HII}	(10^2 cm^{-3})	0.8 – 3	0.9
	r_{HII}	(pc)	0.08 – 0.2	0.08
unif. ring	n_{rg}	(10^3 cm^{-3})	1 – 2	1
	r_{rg}	(pc)	0.16	0.16
	w_{rg}	(10^{17} cm)	0.7 – 2	1.7
	h_{rg}	(10^{16} cm)	3.5	3.5
clumps	$< n_{cl} >$	(10^4 cm^{-3})	1 – 3	2.2 – 2.8
	$< r_{cl} >$	(pc)	0.14 – 0.17	0.14 – 0.17
	w_{cl}	(10^{16} cm)	1 – 3	1.7
	N_{cl}		40 – 70	50

Synthesis of the X-ray emission

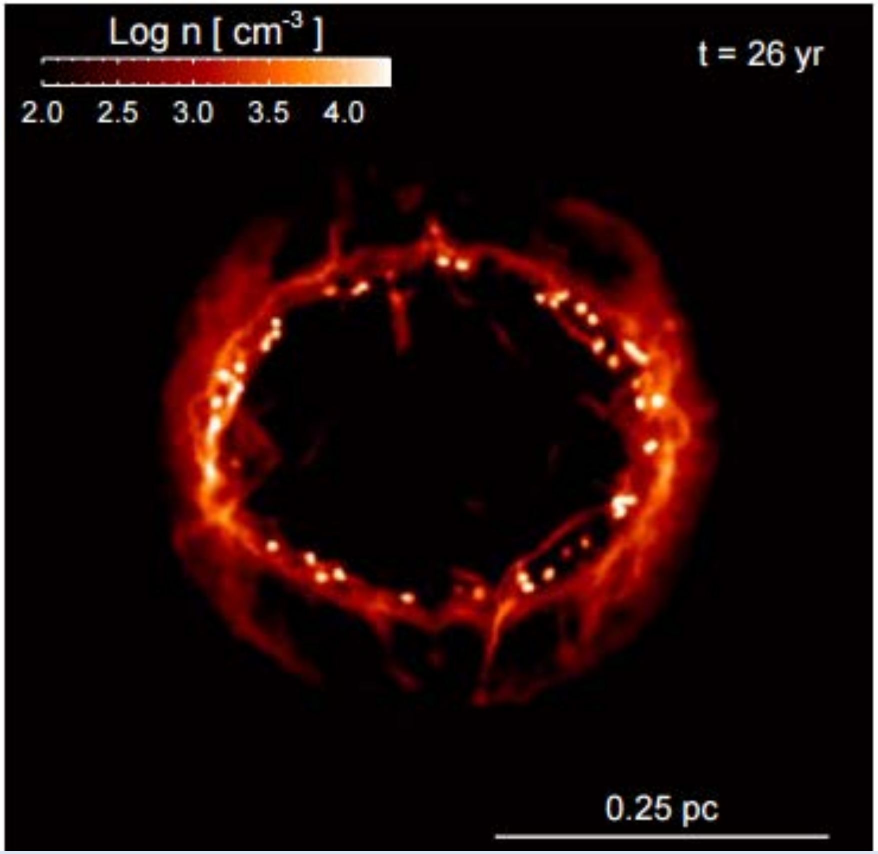

By adopting **ATOMDB V3.0,** we derive the synthetic X-ray emission in each computational cell from

- Electron/proton temperature (including p^+-e^- Coulomb collisions)
- Plasma density
- Time elapsed after the shock heating

Abundances Zhekov+ (2009)

ISM Absorption: 2.3e21 cm^{-2}(Park+2006)

Distance: 1.4 kpc (Panagia 1999)

The synthetic emission is then **folded through the instrumental *XMM-Newton* and *Chandra* responses**

Synthetic fluxes and images

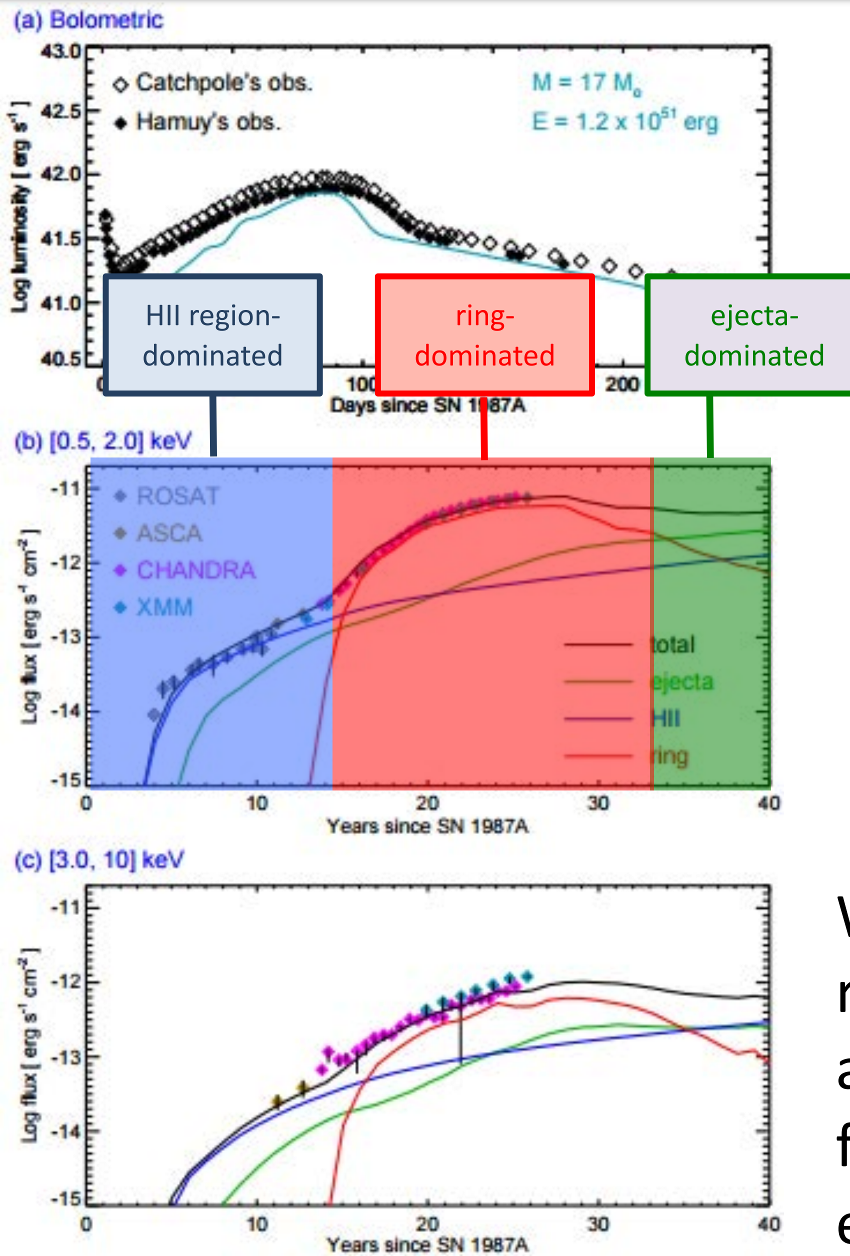

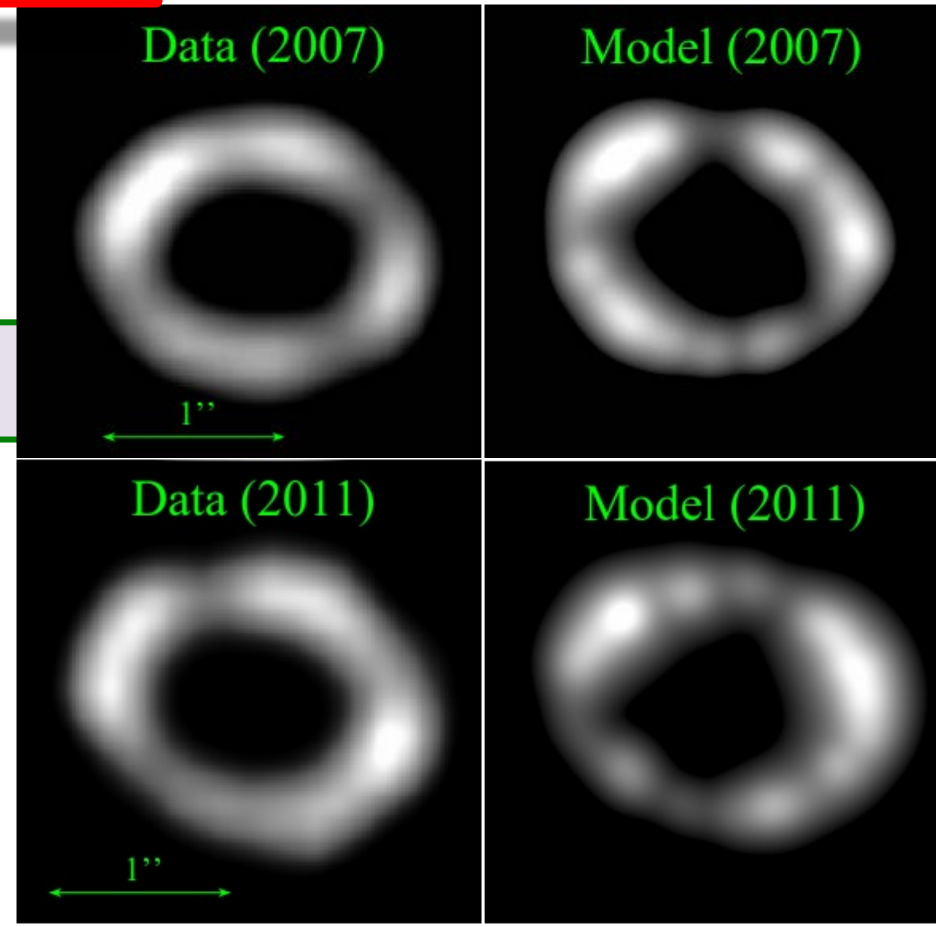

We also found T_e/T_p=0.16 at the reverse shock (in 2011), in agreement with T_e/T_p=0.14-0.35 from HST-COS observations (France et al.2011)

Synthetic X-ray spectra (CCD)

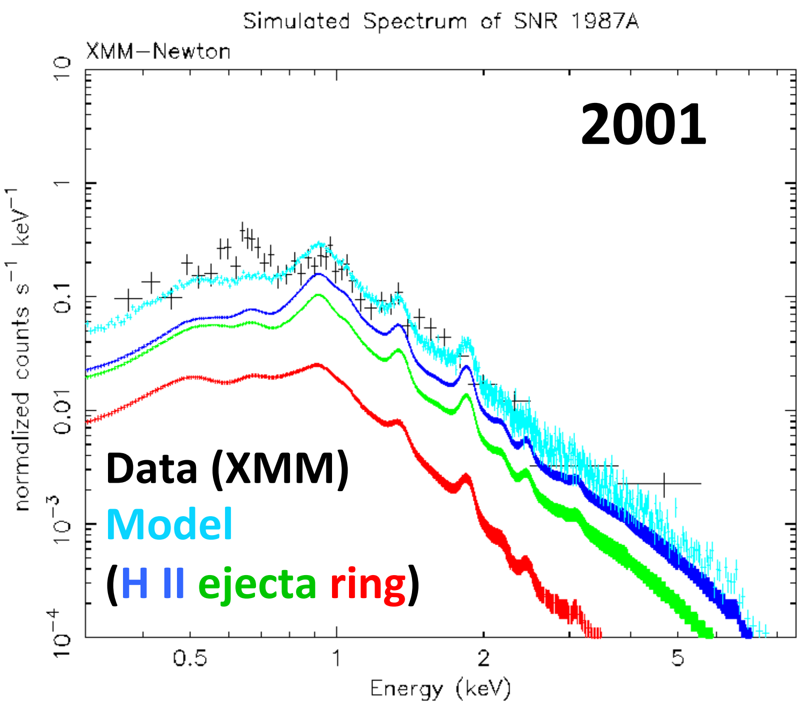

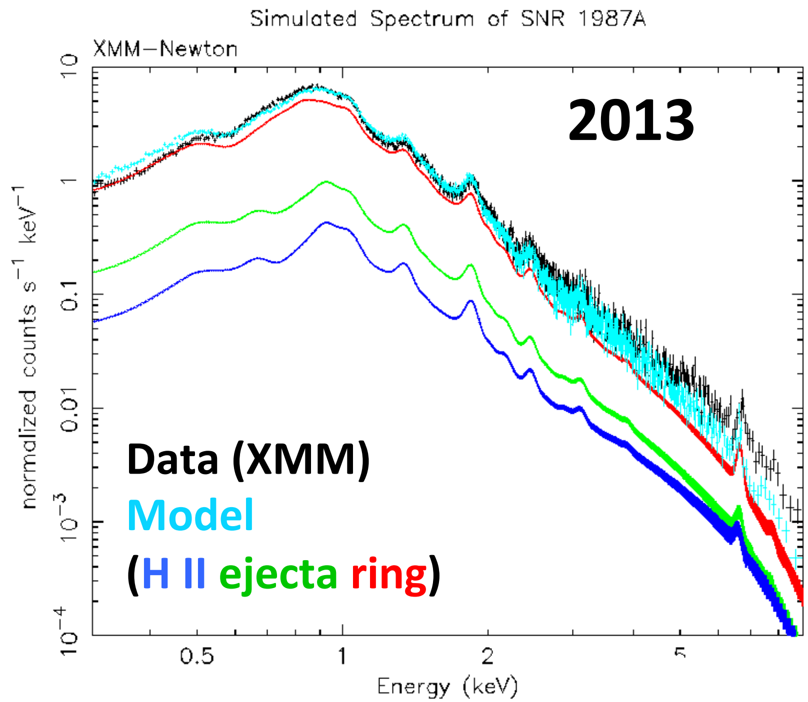

A **single hydrodynamic model** that **accounts self-consistently** for all the available X-ray observations (and for the evolution of the system) and provides unique information on the physical origin of the X-ray emission

Synthetic high-resolution X-ray spectra (gratings)

We included all the possible sources of line broadening:

- **Bulk velocities** of the different parts of the ring
- **Spatial extension and instrumental broadening** (due to both line response function and X-ray source dimension in the dispersion direction)
- **Thermal broadening**

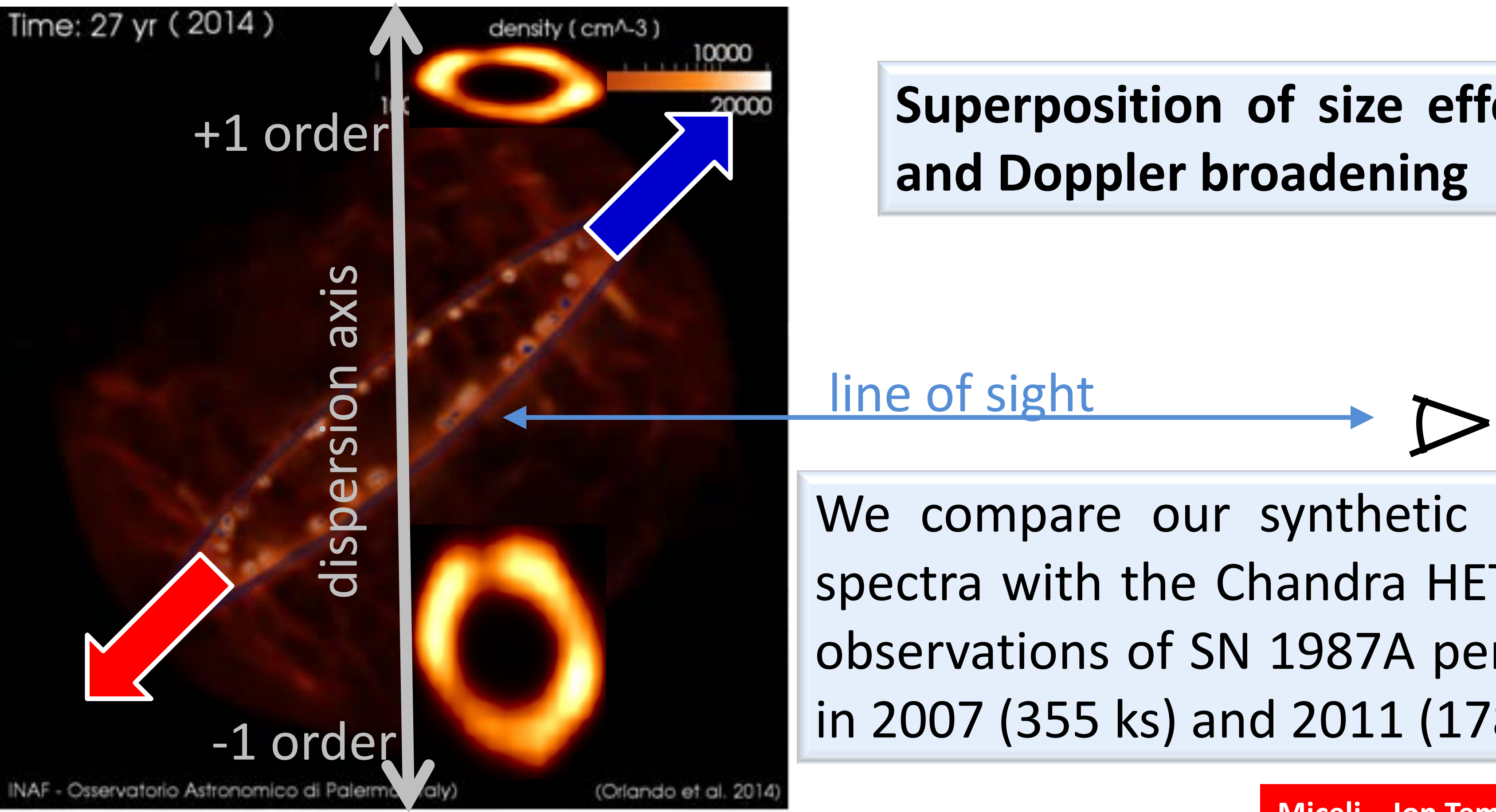

Superposition of size effects and Doppler broadening

We compare our synthetic gratings spectra with the Chandra HETG MEG observations of SN 1987A performed in 2007 (355 ks) and 2011 (178 ks)

Synthetic high-resolution X-ray spectra (gratings)

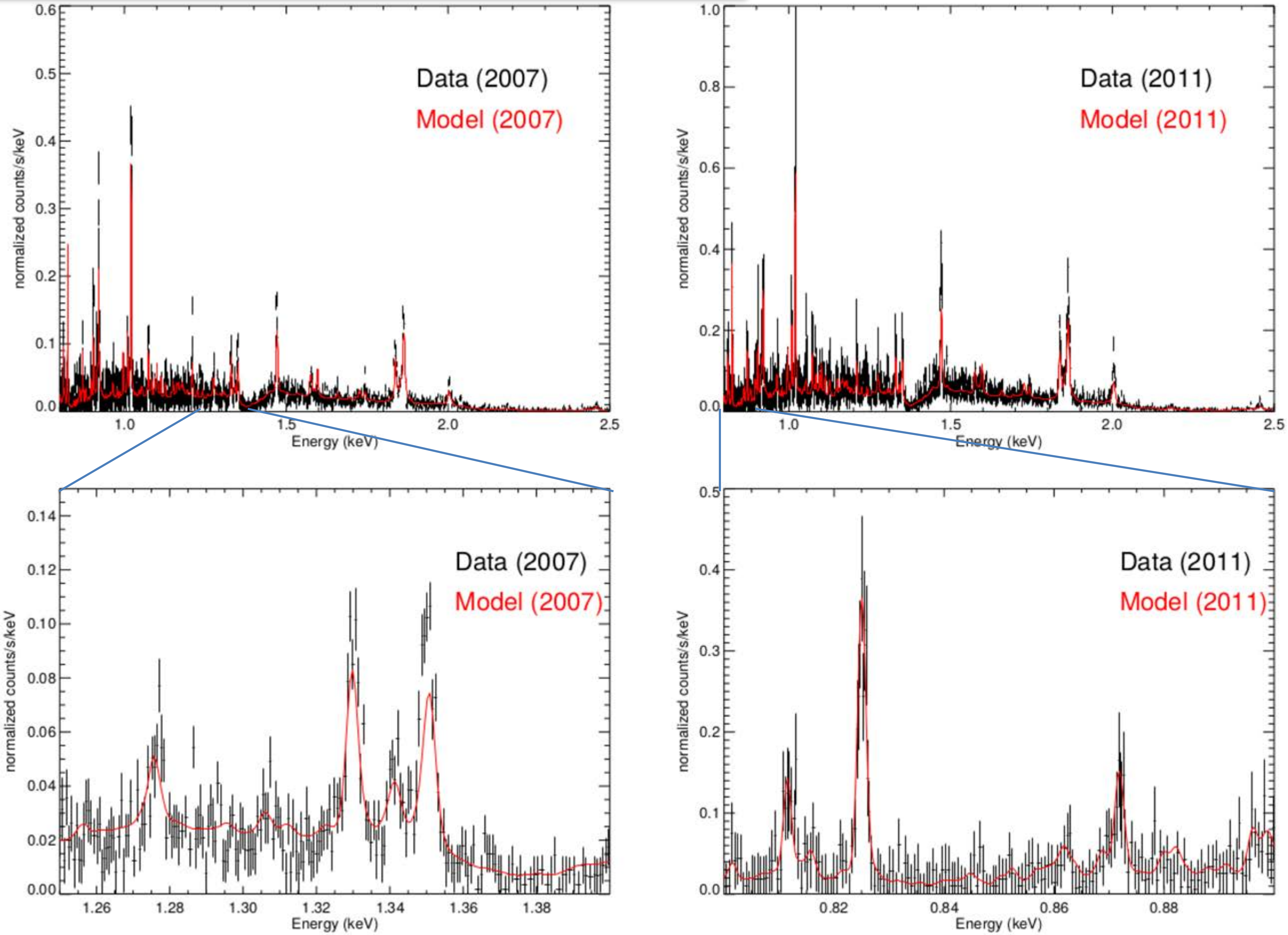

Miceli et al. 2019, Nat. Astron. 3, 236

X-ray line broadening

We can turn ON/OFF thermal broadening in our synthetic spectra and compare the model line widhts with actual data. The broadening due to **Doppler shift and the angular size of the source cannot reproduce the observed line widhts**. The addition of thermal broadening naturally reproduces the observations

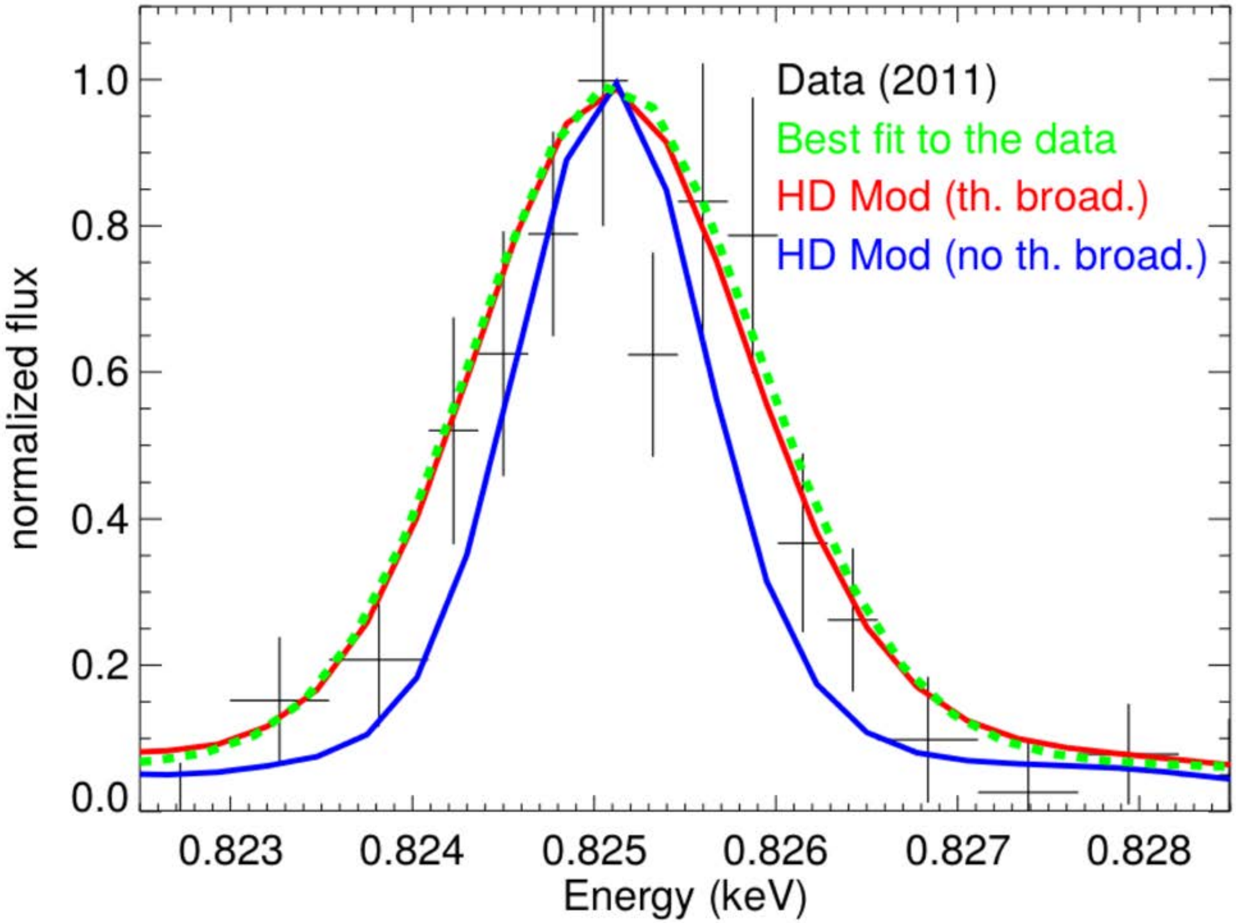

Miceli et al. 2019, Nat. Astron. 3, 236

X-ray line broadening

Doppler shift and the angular size of the source cannot reproduce the observed line widhts. The addition of thermal broadening naturally reproduces the observations for all the emission lines at different epochs

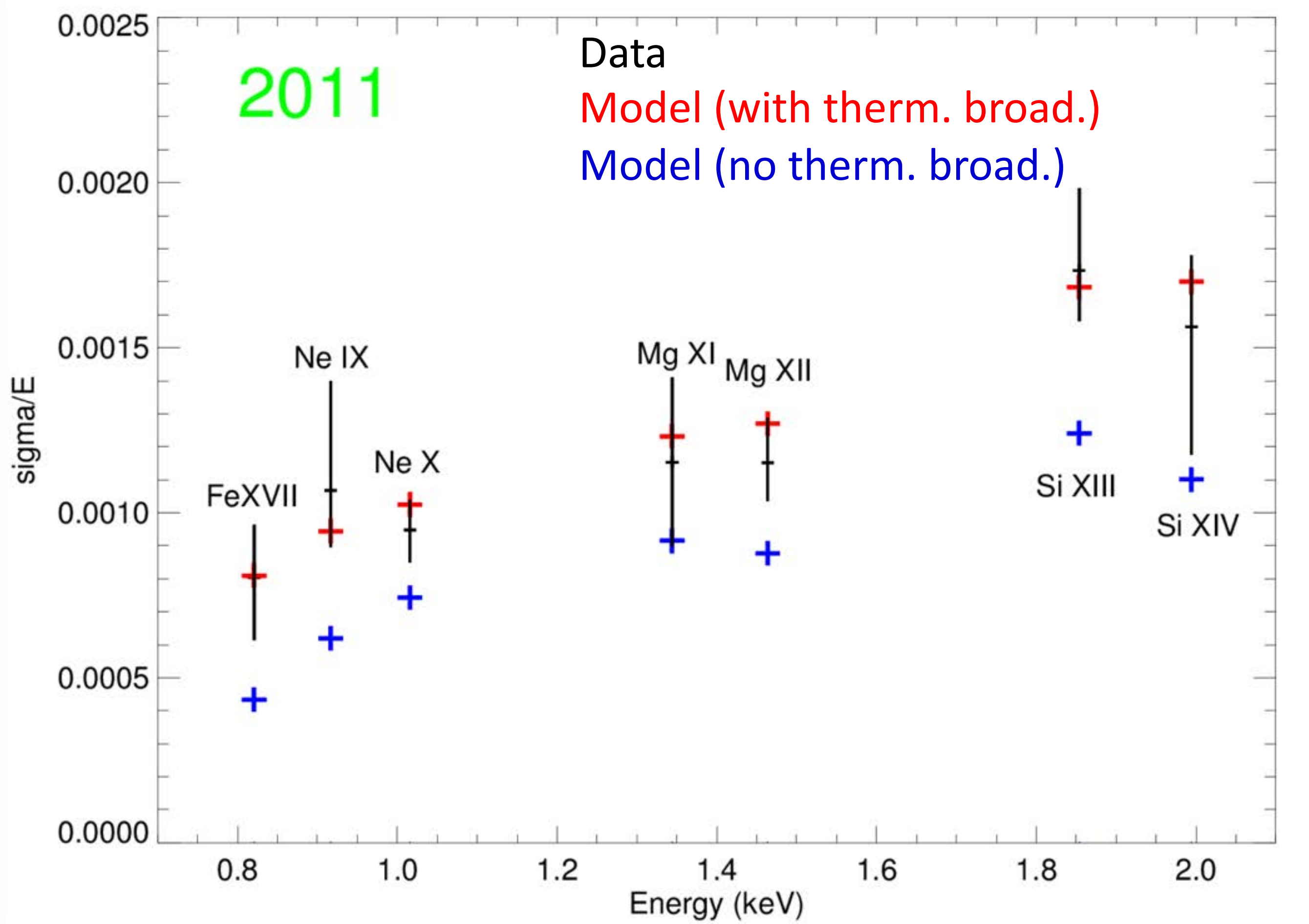

Miceli et al. 2019, Nat. Astron. 3, 236

Ion temperatures derived from the line widths

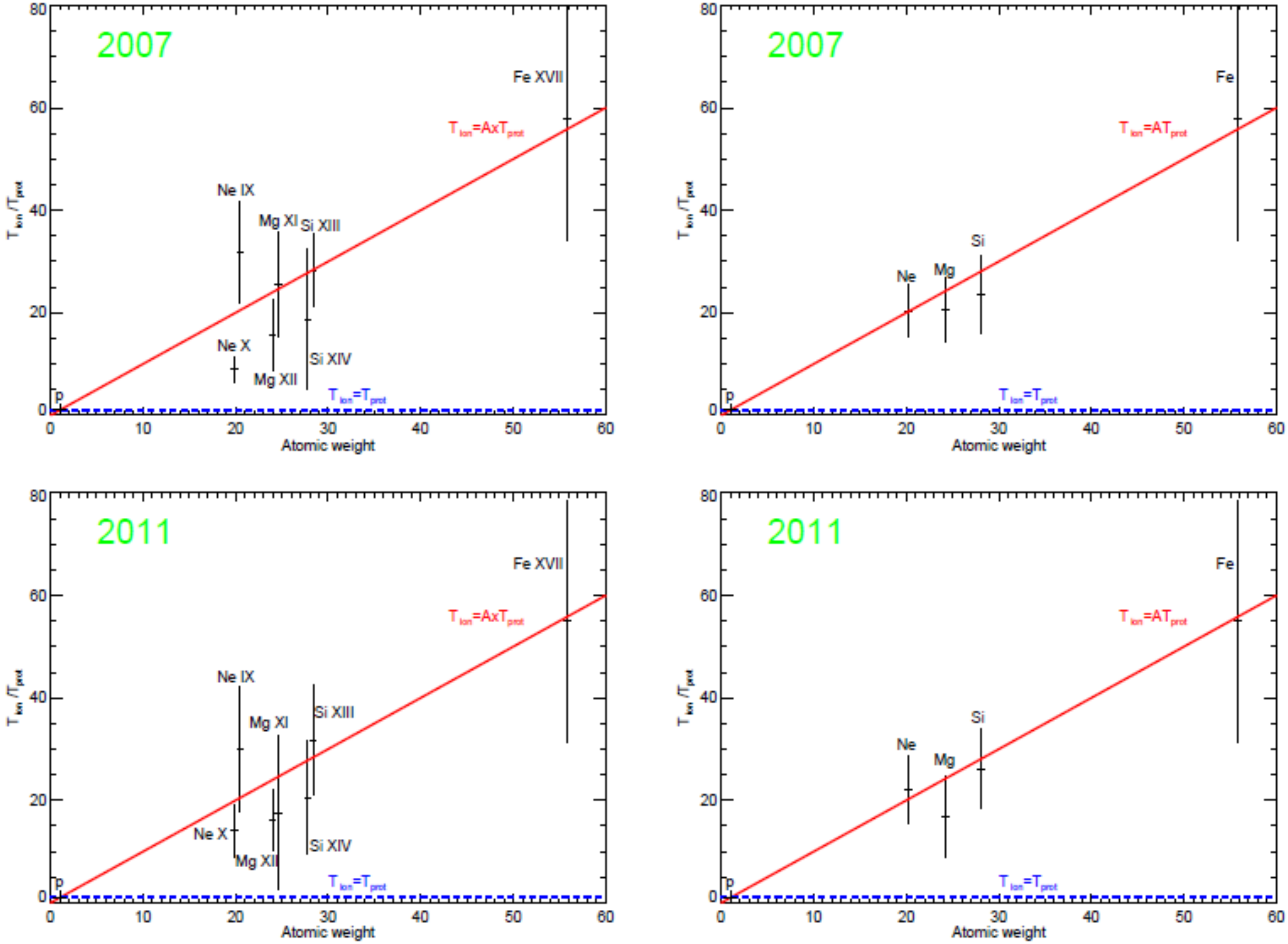

Miceli et al. 2019, Nat. Astron. 3, 236

Ion temperatures derived from the line widths

By comparing the observed line width with that derived from the model without thermal broadening we can measure the ion temperatures

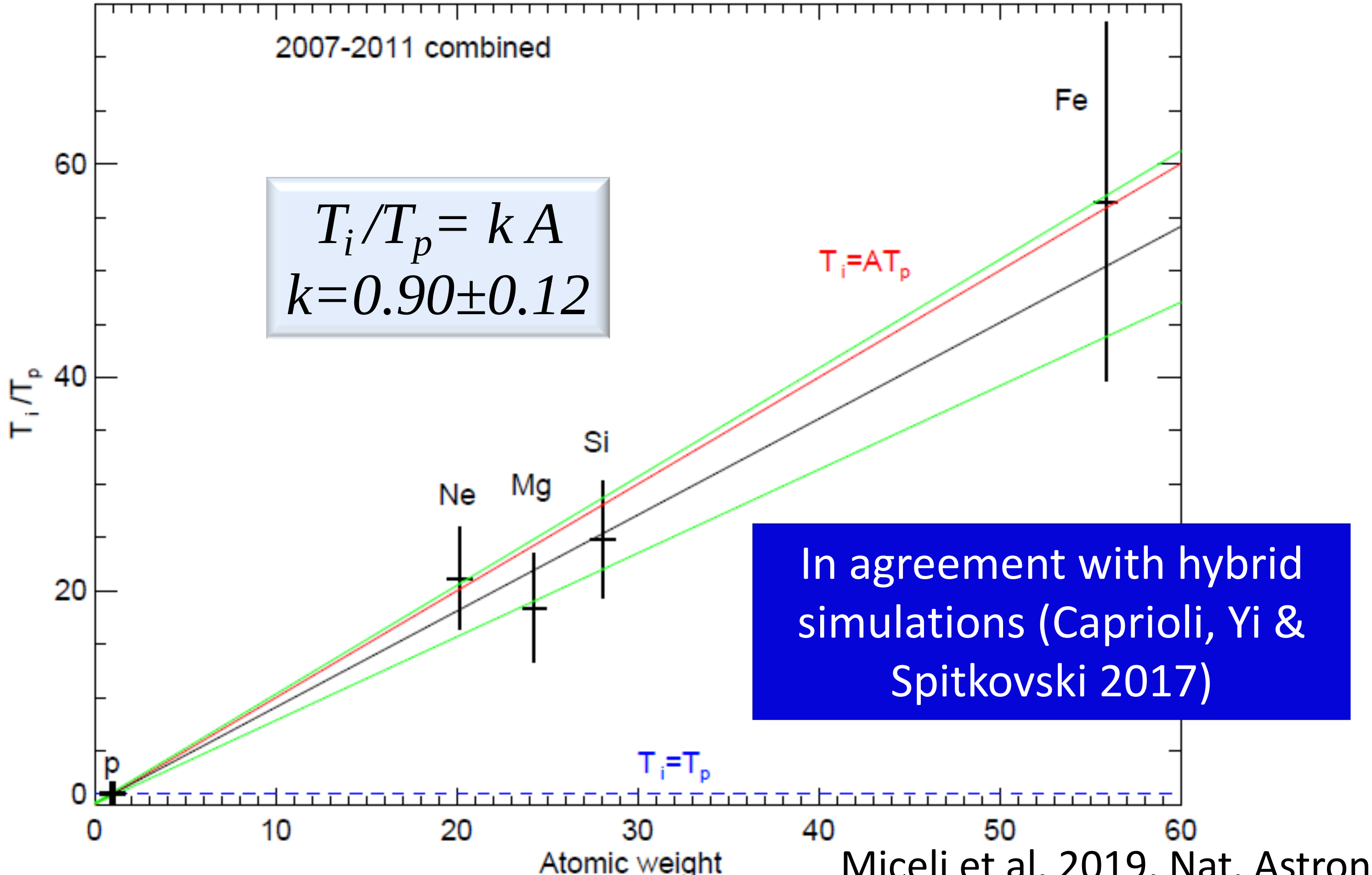

Miceli et al. 2019, Nat. Astron. 3, 236

best fit (simple linear regression)

90% error bars

Ion temperatures derived from the line widths

We performed the same analysis on the 2018 Chandra deep observation of SN 1987 A (see **poster S10.16 by A. P. Ravi** for further details)

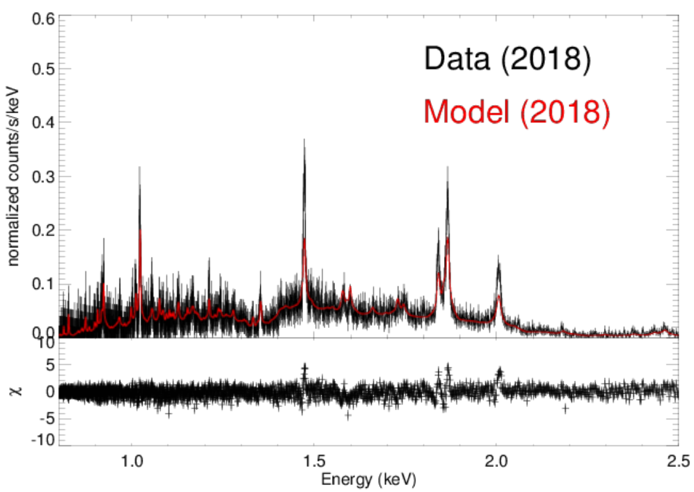

The model still reproduces the observed spectra

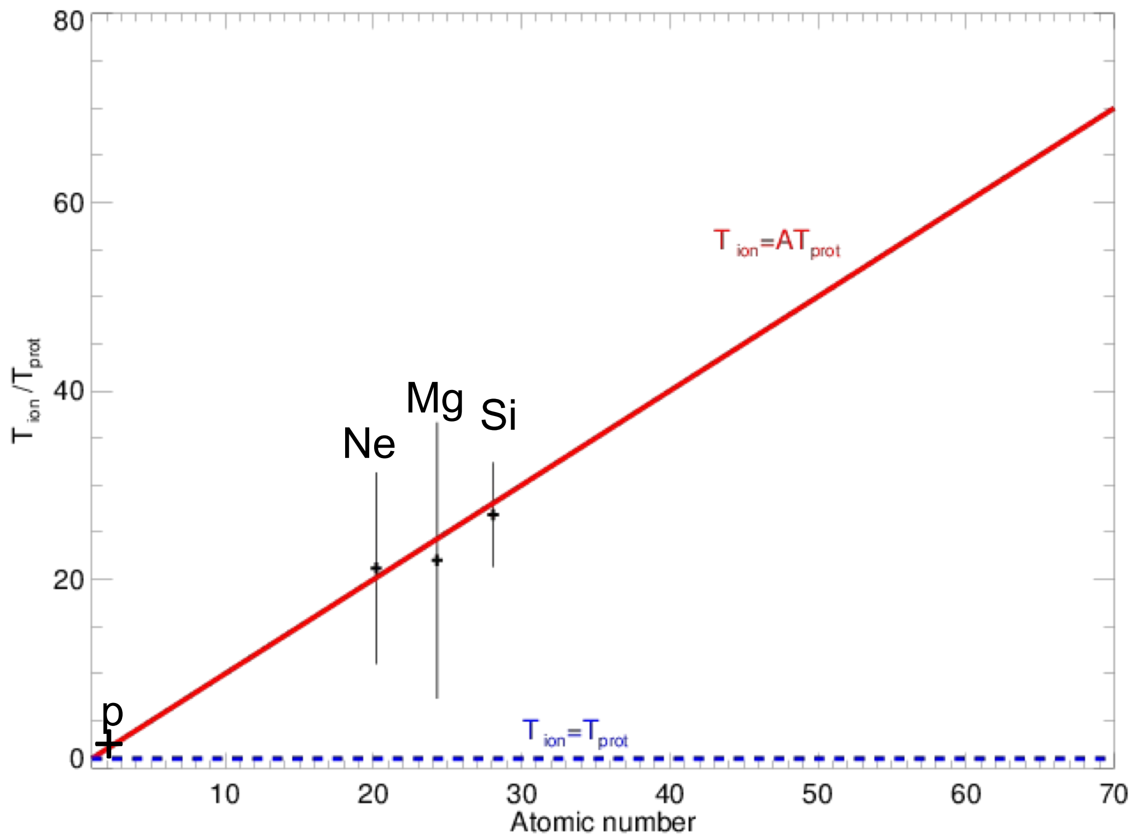

The mass proportional trend is confirmed by the new data (error bars are a little bit larger because of the relatively low statistics)

Conclusions

We studied the collisionless shock heating in SN 1987A with a unique hydrodynamic model that accounts self-consistently for all the X-ray observations performd so far. The synthesis of observables from the HD simulations and the comparison with the data allowed us to:

- Test the model (accurate description of the SN-CSM interaction)
- Get a deep physical insight on the origin of the observed emission
- Ascertain the role of the Doppler and thermal broadening in shaping the X-ray line profiles
- Accurately measure the ion temperatures
- Derive the relationship between kT_i and m_i for an unprecedentedly wide range of masses (from Ne to Fe)

For further details:
Miceli et al. 2019, Nature Astronomy 3, 236, publicly available at https://rdcu.be/bhO7Z